

A Novel Sensitive and Selective Amperometric Detection Platform for the Vanillin Content in Real Samples

Serkan Karakaya^{*,[a]} and İsmet Kaya^[a]

Abstract: Accurate and sensitive determination of vanillin in commercial samples is significant for food safety & quality. In the proposed study, copper particles were coated on an indium tin oxide electrode (ITO) by cyclic voltammetry (CV) for the determination of vanillin in food samples. CV studies indicated that the electro-deposition of Cu particles provides a good electrocatalytic

effect towards the oxidation of vanillin. The fabricated sensor determines vanillin linearly between 0.50 μM –2.0 mM (Limit of detection: 0.15 μM). The Cu/ITO was successfully tested on vanillin samples and the recommended method provides accurate and selective determination of vanillin in daily samples.

Keywords: Vanillin, Food Safety · Cu Particles · Electrochemical Sensor · Sensors.

1 Introduction

Vanillin, known as 4-hydroxy 3-methoxy benzaldehyde is the main constituent of the *Vanilla planifolia* orchid herb and it is primarily obtained from vanilla pods or beans. Vanillin is widely used in enhancing the flavor of various food products such as wine, ice cream, candy, etc. [1]. On the other hand, vanillin may cause allergic reactions and the health condition of migraine sufferers may be aggravated [2]. Excess intake of vanillin can cause kidney and liver function by leading to some symptoms such as vomiting, headaches, and nausea [1]. The intake of vanillin by the United Nations Food and Agriculture Organization was reported as <10 mg/kg per day [2]. So the development of reliable and fast techniques for the determination of vanillin is necessary for food and pharmaceutical analysis [3]. Therefore, the use of analytical sensors is very significant for controlling food safety in the food industry [4,5]. Analytical methods accurately enable the separation and determination of vanillin content. Electrochemical techniques are cost-effective and more reliable for quality control [3]. Also, electrochemical techniques receive significant attention due to their unique properties such as high selectivity, low cost, sensitivity, operational simplicity, and fast response [1,6–8]. Over the last ten years, the quick development in the electrochemical determination of vanillin has become a new choice [9–15].

A semiconductor material, indium tin oxide (ITO), is a widely used working electrode used in electrochemical sensing and solar cells due to its suitability in various solvents [16]. Moreover, ITO is accepted as one of the furthest used transparent conductive oxides in optoelectronics owing to its well electrical conductivity and superior optical transparency [17]. ITO has been utilized as a disposable working electrode in electrochemical sensing because of its stable electrochemical performance, wide working potential, low cost, and mass produc-

tion [18]. The modification material plays a key role in the electrochemical detection of vanillin by affecting selectivity and sensitivity. Therefore, new electrode modifiers are essential to detect vanillin accurately and quickly [5]. Metal nanoparticles were recognized for their excellent electrocatalytic properties in the electrochemical detection of many important analytes [19,20]. Compared with some other metal nanoparticles (Au, Ag, and Pt) modifiers used in the fabrication of sensors and biosensors, Cu particles are cheaper and exhibit better electrocatalytic properties [21]. Besides, Cu originated nanomaterials enhance the sensitivity due to their unique properties such as superior conductivity, efficient electron transfer, and good mechanical strength [22,23].

In this work, Cu particles have been decorated on ITO (Cu/ITO) for the amperometric detection of vanillin for the first time. The fabricated sensor selectively determines vanillin in presence of many possible interferences and the proposed method enables accurate, sensitive, and selective detection of vanillin in samples.

2 Materials and Methods

2.1 Chemicals and Apparatus

Vanillin ($\text{C}_8\text{H}_8\text{O}_3$, 99 %, 152.15 g mol^{-1}) was procured from Alfa Aesar. CH_3COOH , $\text{Cu}(\text{NO}_3)_2 \cdot 5\text{H}_2\text{O}$, D(-)-fructose, H_3BO_3 , H_3PO_4 , $\text{K}_4[\text{Fe}(\text{CN})_6] \cdot 3\text{H}_2\text{O}$, KCl, $\text{K}_3[\text{Fe}(\text{CN})_6]$, KNO_3 , MgCl_2 , $\text{NaCH}_3\text{COO} \cdot 3\text{H}_2\text{O}$, Na_2CO_3 , NaNO_3 , NaOH, and Na_2SO_4 were supplied from Merck.

[a] S. Karakaya, İ. Kaya

Polymer Synthesis and Analysis Laboratory, Department of Chemistry, Faculty of Science and Arts, Çanakkale Onsekiz Mart University, 17100 Çanakkale, Turkey
Phone: +902862180018/22254
E-mail: skarakaya@comu.edu.tr

Sucrose was purchased from FG bioscience. D(+)-mannose and D(+)-maltose monohydrate were purchased from Across Company. D-(+)-Glucose was supplied from Sigma-Aldrich. A water purification system Millipore direct Q3 with a UV lamp was used to obtain ultrapure water for the preparation of all solutions. The pH values of buffer solutions were arranged with a HI 221 Hanna-HI-1332 pH-meter. The electrochemical studies were performed with a CHI 660C model workstation device (CH Instruments from Texas, USA). An electrode system containing a reference electrode (BASi Ag vs. AgCl_(sat. KCl)), a counter electrode (BASi Pt wire), and a working electrode (ITO) were used to perform all electrochemical measurements. ITO coated PET as procured from Sigma-Aldrich. A 1.0 cm² of ITO was used in all electrochemical measurements.

A Zeiss/EVO 40 equipped with EDAX: Ametek device was used to record the SEM micrographs and EDX spectra of the bare and modified electrodes. XRD patterns of the electrodes were examined by an XRD PANalytical Empyrean device.

2.2 Modification Procedure for Cu Decorated ITO

A previously published procedure was modified to fabricate the vanillin sensor [23]. Copper particles were modified on ITO by recording the CVs of 10.0 mM Cu(NO₃)₂·5H₂O containing 0.10 M KNO₃ for 5 successive cycles at a scan rate of 100 mV/s and a potential range of -0.70 V–+0.80 V).

2.3 Electrochemical Analysis

Electrochemical impedance (EI) curves of ITO and Cu/PGE were taken in 0.005 M Fe(CN)₆^{3-/4-} solution including 0.10 M KCl (Frequency range: 0.10–100000 Hz). Cyclic voltammetric behavior of the ITO and Cu/PGE were analyzed towards 1.0 mM vanillin in pH 9.0 BRB solution including 0.10 M KCl. The pH and scan rate effects on oxidation of vanillin were tested towards vanillin (1.0 mM) by the CV method. The best condition for applied potential was optimized as +0.85 V. Amperometric responses of both ITO and Cu/ITO were investigated in presence of increased concentrations of vanillin (Applied potential: +0.85 V and constant stirring: 800 rpm).

2.4 Applicability Studies

Applicability of the vanillin sensor was tested on vanillin syrup (3.00 %) and vanillin powder (25.00 %), which were supplied from a local market. Vanillin powder was dissolved in 100 mL of pure water. Vanillin syrup and vanillin powder samples were diluted with pH 9.0 BRB in ratios of 1:10000 and 1:100 in an electrochemical cell and standard additions of 100 μM of vanillin was made.

3 Results and Discussion

3.1 Preparation of the Vanillin Sensor

Figure 1 shows the recorded CVs for the electrodeposition process of copper particles on ITO. It was found that the CVs obtained in this work were quite similar to those obtained in the literature [24,25]. Differently, Au and Cu trifluoromethylsulfonate (Cu(TFO)₂) in 1-butyl-3-methylimidazolium trifluoromethylsulfonate ([BMIm][TFO]) solution was used as the working electrode and supporting electrolyte solution in these studies, respectively. A redox couple (a₂/c₂) can be seen from Figure 1. Two peaks (a₁ and a₂) observed at +0.46 V and +0.65 V in the anodic scan can be attributed to the Cu⁰→Cu⁺ and Cu⁺→Cu²⁺, respectively [24,25]. “c₂” in the cathodic scan (near at -0.70 V) is related to the reduction of Cu²⁺→Cu⁺, and this reduction state starts at 0 V [24,25]. This means that the Cu particles form as Cu₂O on ITO (Proved by XRD analysis). The peaks (at +0.46 V and +0.65 V) seen at the first scan shifted to more positive potentials and the current increased by the increase of cycles at both anodic and cathodic regions (Figure 1). The changes in CVs reflected that the modification of Cu particles occurred on ITO.

3.2 Characterization Studies

To examine the electrochemical characterization of the Cu/ITO, electrochemical impedance (EI) curves of the bare and modified electrodes were recorded (Figure 2). EI spectroscopy is extensively used for the examination of the surface conductivity properties of the electrodes. The semi-circle diameter of an EI curve gives charge transfer resistance (R_{ct}) which is directly related to surface conductivity properties. When the EI curves were taken to consider for both electrodes, R_{ct} is quite high at bare ITO (840 Ω) due to the poor electron transfer between ITO and Fe(CN)₆^{3-/4-}. On the other hand, R_{ct} (140 Ω) significantly decreased after modification of Cu particles

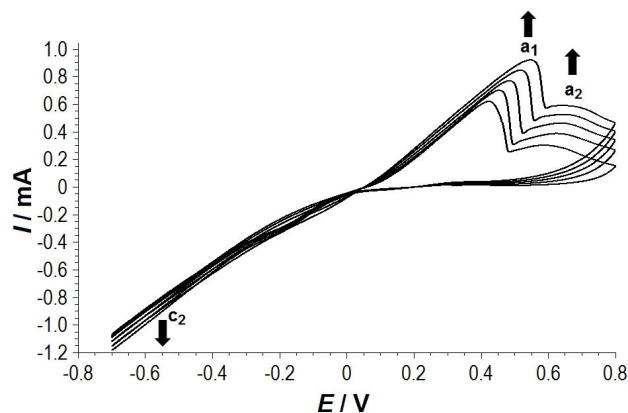


Fig. 1. Five sequential CVs recorded at ITO in 10.0 mM Cu(NO₃)₂·5H₂O including 0.10 M KNO₃ at a scan rate of 100 mV/s and a potential range of -0.70 V–+0.80 V).

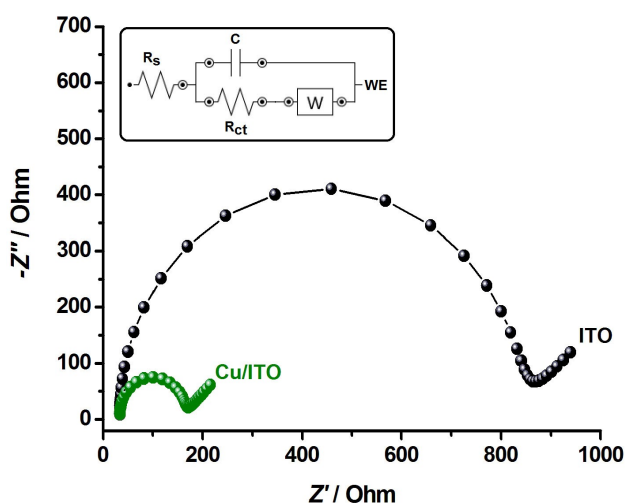


Fig. 2. The EI curves for Cu/ITO and bare ITO recorded in 0.005 M $\text{Fe}(\text{CN})_6^{3-/4-}$ solution including 0.10 M KCl (Frequency range: 0.10–100000 Hz, impedance circuit model in the inset: “C” as double-layer capacitance, “WE” as working electrode, “W” as Warburg impedance, and “ R_s ” as ohmic resistance).

onto ITO due to the good conductivity properties of Cu particles.

Surface morphologies of the electrodes were analyzed by recording their scanning electron microscopy (SEM) images (Figure 3A and 3B), energy-dispersive X-ray (EDX), and X-ray diffraction (XRD) spectra (Figure 3C and 3D) to obtain further evidence for deposited Cu particles on ITO. SEM images indicated that the smooth surface morphology of bare ITO completely changed after the electrodeposition of Cu particles. The recorded SEM images showed that Cu particles are positioned almost cubically on the ITO surface. The Cu particle dimensions were found within the interval of 226–345 nm. The EDX spectra of both electrodes also showed that differently from the signals (42.48% C, 37.73% O, 4.81% Au, and 14.98% In) for bare ITO, after Cu particles were electrodeposited, one additional Cu signal (7.20%) observed. The XRD patterns of both electrodes were further examined (Figure 3E). The diffraction peak observed at 2θ degrees of 36.5 for Cu/ITO indicates (111) planes of Cu_2O which is in good agreement with the literature [26–28]. All the certain changes observed in EIS and morphological studies prove the modification of Cu particles as Cu_2O onto ITO.

3.3 Optimization Studies for the pH and Cycle Number

The optimum conditions for pH and cycle numbers related to the amount of Cu particles deposited on ITO were optimized. Firstly, the best condition for pH was optimized in various pH values of the Britton Robinson buffer (BRB) solution. For this aim, CV responses of 1.0 mM vanillin at Cu/ITO were recorded at different pH values (8.0–10) of the BRB solution (Figure 4A). It is

observed that as the pH increases, the peak potential of vanillin seen at the anodic region shifts to the negative direction. The response towards oxidation of vanillin was found to be very weak and observed as broad peak at pH 8.0. On the other hand, the peak current belongs to the oxidation of vanillin enhanced between 8.0 and 9.0. This response significantly decreased after pH 9.0 (at pH of 9.5 and 10). Due to the best response observed at 9.0, this value was chosen as the most suitable pH for the BRB solution. The linear relationship between the pH and peak potential of vanillin was also given in Figure 4B. The obtained slope 0.062 V/pH near to Nernstian slope (0.059) supports that the equal numbers of H^+ and e^- take part in the electrocatalytic oxidation of vanillin.

The cycle number related to the amount of Cu particles deposited on ITO was further optimized. For this aim, Cu particles modified ITO electrodes were prepared with various cycles (3, 5, 7, 10, and 15), and the electrochemical response of 1.0 mM vanillin at prepared electrodes was tested by CV. The obtained cycle number vs. peak current plots suggests that the highest response was obtained with 5 cycles (Figure 5). The Cu/ITO prepared with 5 cycles was chosen as the most suitable electrode for further studies.

3.4 The Examination of the Scan Rate Effect

The scan rate effect on the response of vanillin was also investigated. It is obvious from the CVs that the electrochemical response enhances by the increase of scan rate between 10–500 mV/s (Figure 6A). The obtained high linear relationship ($R^2=0.9939$) between the square root of the scan rate and peak current suggests that the electrochemical oxidation on Cu/ITO occurs by diffusion-controlled (Figure 6B).

3.5 Cyclic Voltammetric Response of the Vanillin Sensor

Electrochemical response at both ITO and Cu/ITO was tested in the absence and presence of 1.0 mM Vanillin by CV (Figure 7A). As expected, unmodified ITO shows electrochemically inactive behavior in absence of vanillin (Figure 7; blackline, a). At the same conditions, Cu/ITO shows capacitive background curves (Figure 7, green line, c). In the presence of vanillin, the oxidation of vanillin requires high potentials (over +1.2 V) at bare ITO (Figure 7; blue line, b). After the modification of Cu particles on ITO, the peak potential shifted to a more negative direction (+0.85 V) and the oxidation current significantly increased compared with bare ITO (Figure 7A, red line, d). The changes in CVs prove that Cu/ITO exhibits a good electrocatalytic effect towards oxidation of vanillin by both decreasing the over potential and increasing peak current. This is attributed to the facilitation/acceleration of e^- transfer between ITO and vanillin due to the good conductivity properties of the Cu particles, as confirmed by EI measurements. The new

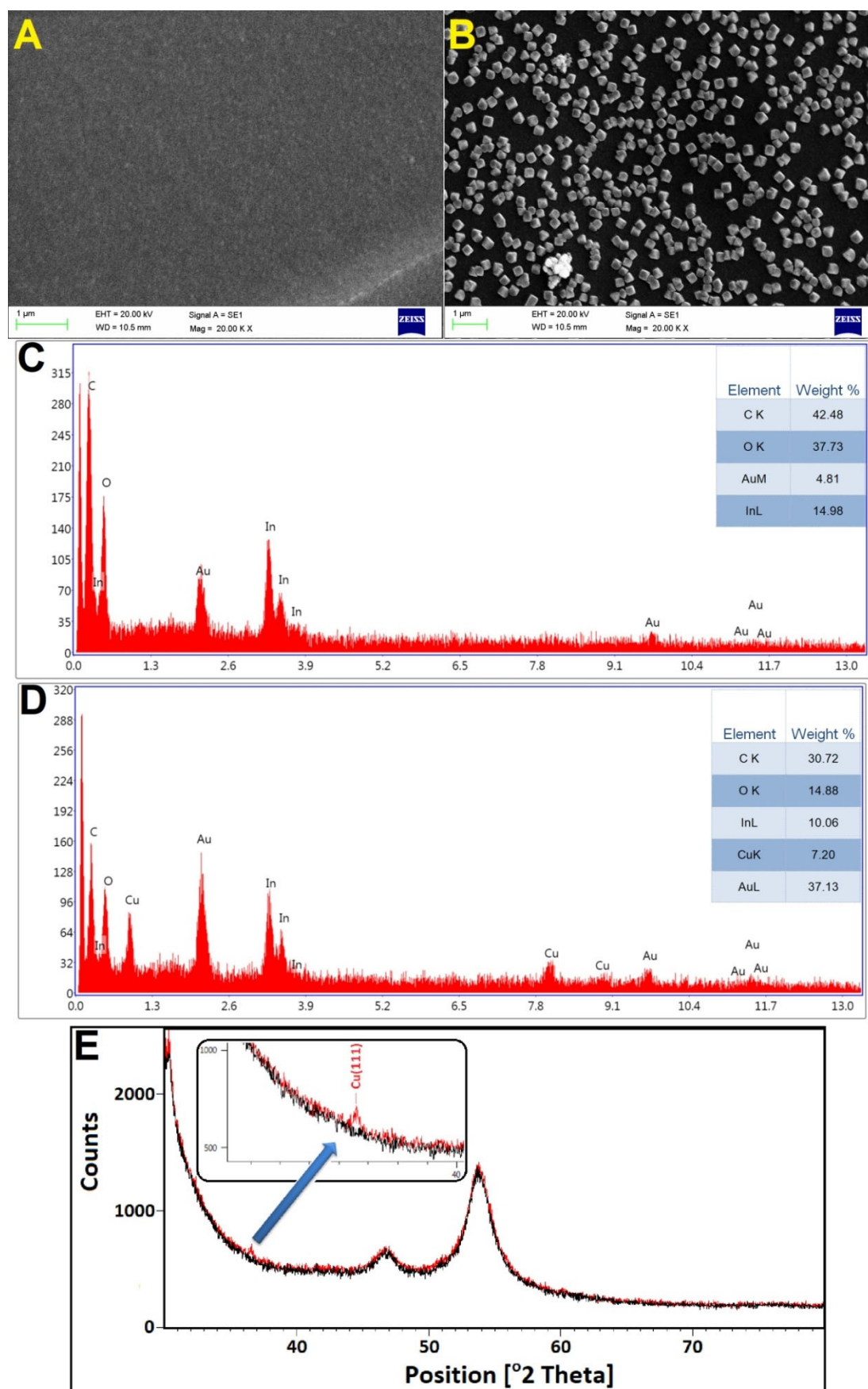


Fig. 3. The SEM micrographs of (A) bare ITO and (B) Cu/ITO (Magnifications: $1.0\ \mu\text{m}$ – $\times 20.00\ \text{K}$), EDX spectra of bare ITO (C) and Cu/ITO (D), and XRD patterns of bare ITO (Black line) and Cu/ITO (Red line).

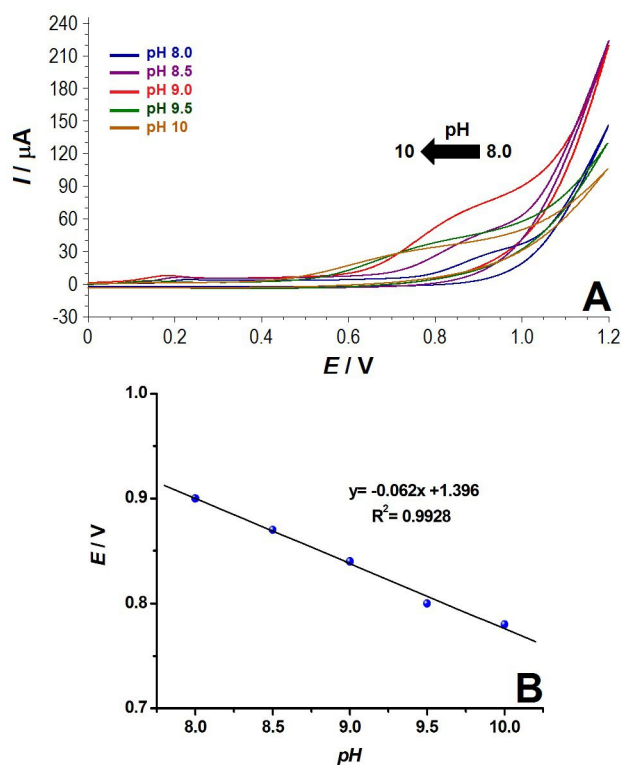


Fig. 4. A) CV responses of 1.0 mM vanillin at different pH values (8.0–10) of BRB solution for Cu/ITO (Scan rate: 50 mV/s and potential range: 0 V–+1.2 V), and B) the linear curve between $E(V)$ and pH ($E(V) = -0.062(pH) + 1.396$ and $R^2 = 0.9928$).

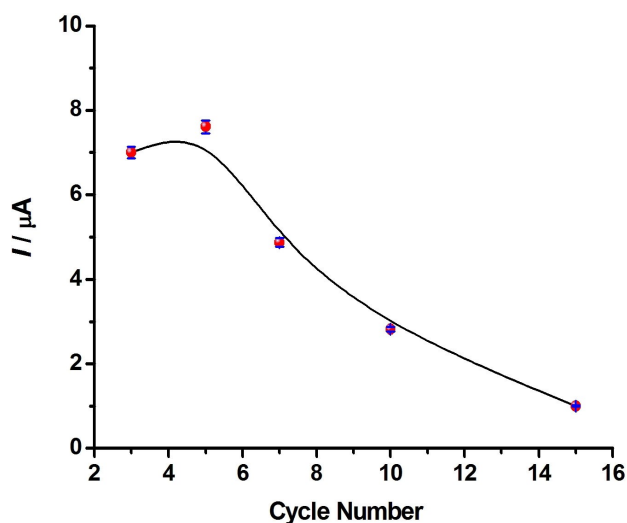


Fig. 5. The peak current vs. cycle number plots obtained for modified electrodes prepared with increased cycles.

surface is more conductive and this may be proposed to explain the enhanced sensitivity toward vanillin detection.

A mentioned mechanism for electrocatalytic oxidation of vanillin at different electrodes was also given (Scheme 1) [29–31]. This mechanism can be also taken into consideration for Cu/ITO. In this mechanism, meth-

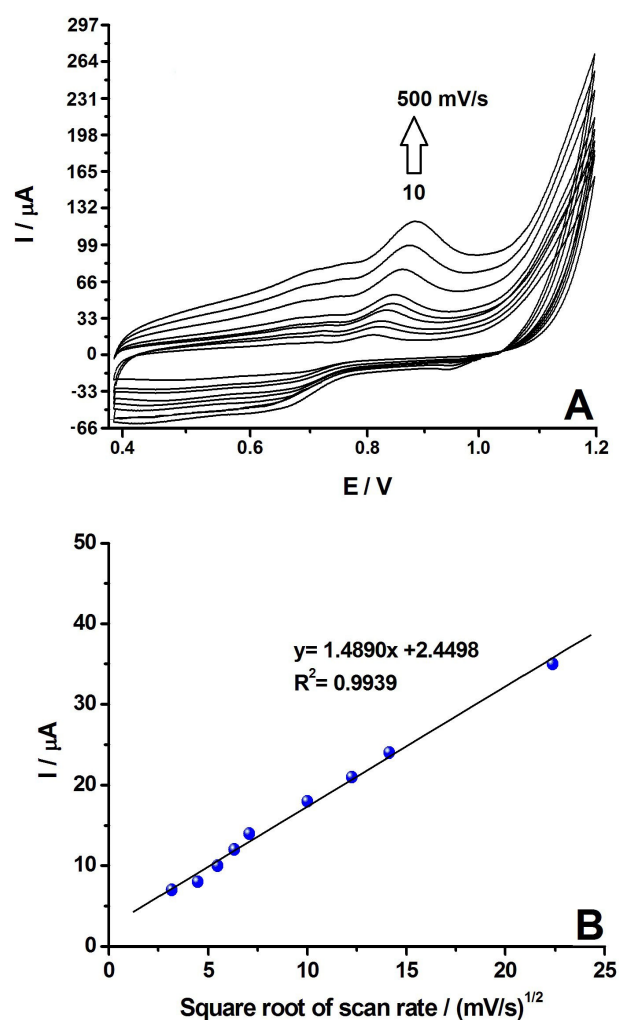


Fig. 6. A) CVs recorded for vanillin (1.0 mM) at increased scan rates (v : 10–500 mV/s) (Potential range: +0.4 V–+1.2 V) and B) the peak current (I) vs. $v^{1/2}$ plots obtained from CVs ($I(\mu A) = 1.4890(v)^{1/2} + 2.4498$ and $R^2 = 0.9939$).

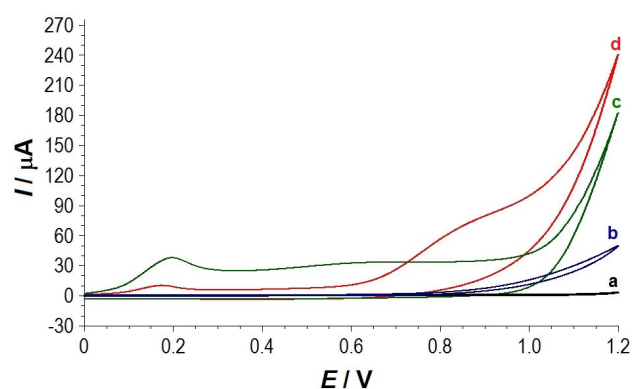
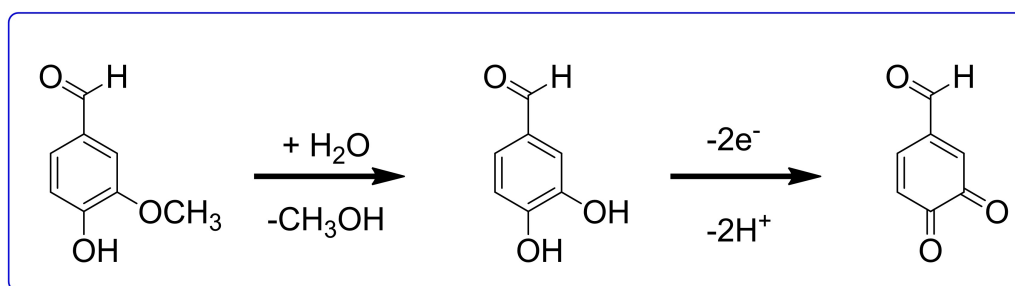


Fig. 7. Cyclic voltammetric responses at (a,b) ITO and (c, d) Cu/ITO in absence (a,c) and presence of (b,d) 1.0 mM Vanillin (Scan rate: 50 mV/s and potential range: 0 V–+1.2 V).



Scheme 1. A mechanism for electrocatalytic oxidation of vanillin.

oxy ($-OCH_3$) substitutes with the $-OH$ group in the basic condition ($pH=9.0$) after an aromatic nucleophilic substitution reaction. Then, the phenolic dihydroxyl groups oxidize to carbonyl ($-C=O$) groups after losing two electrons ($2e^-$) and two protons ($2H^+$) at the redox step.

3.6 The Analytical Performance of Cu/ITO

For the investigation of the analytical performance of the sensor, electrochemical responses of increased vanillin concentrations at both bare ITO and Cu/ITO were examined by amperometry, and the current-time curves were recorded for both electrodes (Figure 8A). Linear response ranges for bare ITO and Cu/ITO were found as $10\ \mu M$ – $1.0\ mM$ and $0.50\ \mu M$ – $2.0\ mM$, respectively (Figure 8B). The limit of detection (LOD) for Cu/ITO was calculated as $0.15\ \mu M$ according to the $3 \times s/m$ (s is the standard deviation for the minimum concentration that gives a signal, and m : the slope of the calibration curve). Repeatability and reproducibility of the sensor were also investigated. Repeatability of the sensor was tested towards 5 successive additions of $10.0\ \mu M$ vanillin and the obtained RSD (3.9 %) from the experiments indicates the proposed vanillin sensor gives highly repeatable responses towards oxidation of vanillin. Reproducibility of the vanillin sensor was examined towards $10.0\ \mu M$ vanillin at 5 individual Cu/ITO electrodes and the RSD of 3.4 % confirms that the proposed sensor exhibits high reproducibility to vanillin.

The proposed vanillin sensor was compared with other published electrochemical vanillin sensors based on their analytical performances. A comparison was given in Table 1. It is clear from the comparison that the proposed vanillin sensor has the largest linear response range, and the LOD of the sensor is lower than many studies [10,12–15]. The better analytical performance of the designed sensor is attributed to the good electrocatalytic and conductivity properties of Cu particles which let efficient electron transfer between Cu/ITO and vanillin.

3.7 Examination of the Selectivity

The selectivity properties of the sensor have been studied in the presence (100 folds) of various types of ionic and molecular interference likely to be found in foods. The

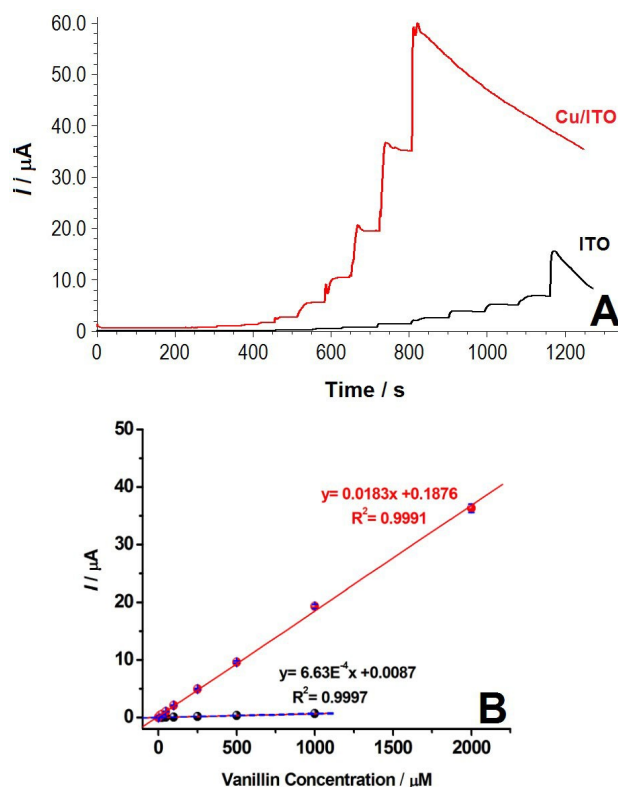


Fig. 8. A) Amperometric responses at ITO (black) and Cu/ITO (red line) at increased concentrations ($10\ \mu M$ – $2.0\ mM$ for ITO and $0.50\ \mu M$ – $3.0\ mM$ for Cu/ITO) of vanillin in pH 9.0 BRB (Applied potential: $+0.85\ V$) and B) the calibration curve obtained for ITO (black line, $I(\mu A) = 6.63E^{-4}C(\mu M) + 0.0087$ and $R^2 = 0.9997$) and Cu/ITO (red line, $I(\mu A) = 0.0183C(\mu M) + 0.1876$ and $R^2 = 0.9991$).

recorded current-time curves confirm that the effect of these ionic and molecular species on the response of vanillin is insignificant (Figure 9). In other words, the proposed sensor can be suitable for selective determination of the vanillin in food samples that include these interferences.

3.8 Analysis of Vanillin Content in Food Samples

The applicability of the vanillin sensor was tested on vanillin syrup and powder samples which were supplied

Table 1. A comparison between the published vanillin sensors and the recommended method.

Type of Electrode	Methodology	LOR	LOD	Ref.
[a] AgNPs/GN/GCE	[f] SWV	2.0–100 μM	0.332 μM	[10]
[b] MoS ₂ -CNF	Amperometry	0.30–135 μM	0.15 μM	[11]
[c] BDD electrode	SWV	3.3–98 μM	0.16 μM	[12]
Cathodically pretreated BDD electrode	[g] SWASV	3.3–330 μM	0.38 μM	[13]
[d] G-QD@Nafion/AuNP-SPCE	[h] DPV	0.66–33 μM	0.32 μM	[14]
[e] CuHCF thin film	CV	0.76–120 μM	0.23 μM	[15]
Cu/ITO	Amperometry	0.50 μM –2.0 mM	0.15 μM	This Work

[a] Silver nanoplates-graphene composite coated glassy carbon electrode; [b] molybdenum disulfide nanoparticles composite coated carbon nanofibers; [c] boron-doped diamond electrode; [d] gold nanoparticle-coated screen printed carbon electrode coated with graphene-quantum dots-nafion; [e] CuHCF: copper hexacyanoferrate; [f] square-wave voltammetry; [g] square-wave adsorptive-stripping voltammetry; [h] differential pulse voltammetry.

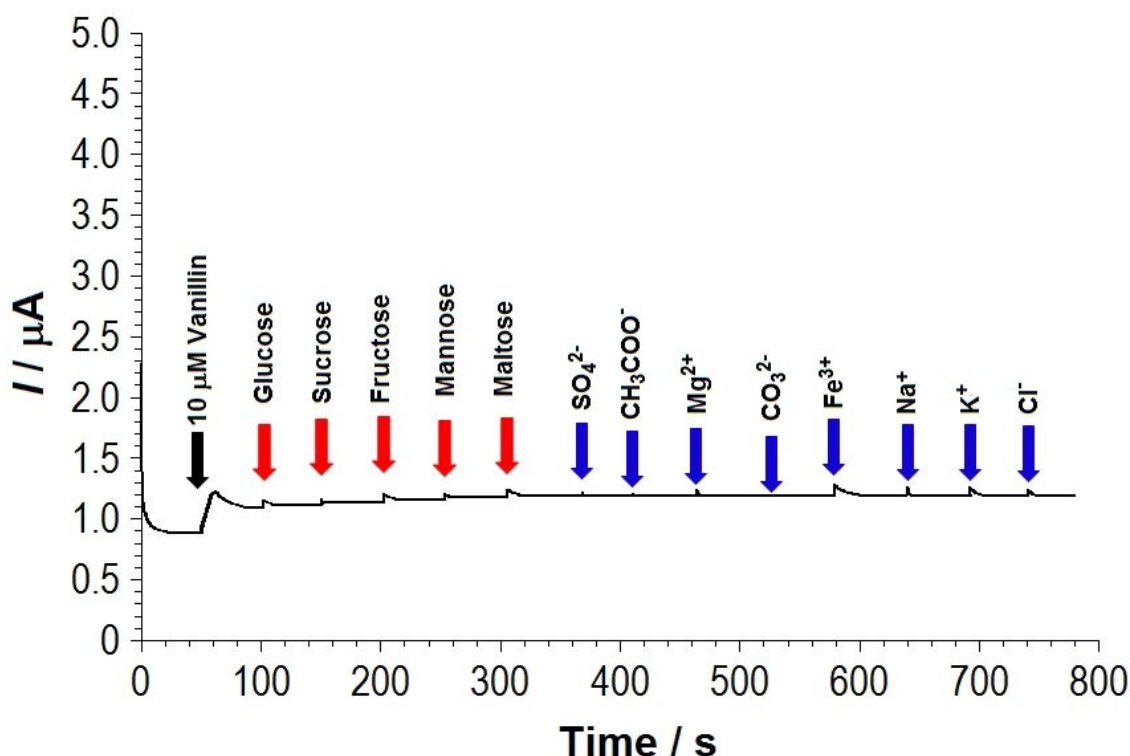


Fig. 9. The current-time graphs obtained towards 10 μM Vanillin in absence/presence of 100 folds (1.0 mM) of various molecular (Glucose, sucrose, fructose, mannose, and maltose) and ionic (SO_4^{2-} , CH_3COO^- , Mg^{2+} , CO_3^{2-} , Fe^{3+} , Na^+ , K^+ , and Cl^-) interferences at Cu/ITO.

from a local market. Vanillin contents of these food samples were found by using both the standard addition-amperometry methods, and the results were compared with those obtained by the UV-Vis method (Table 2).

Statistical analysis of the results for samples was evaluated by statistical *t* and by the *F* tests for comparison of the proposed method and the UV-Vis method. The alternative and null hypotheses are given as H_A : $X_{\text{Average}} = \mu$ and H_0 : $X_{\text{Average}} \neq \mu$ for the *t*-test. μ and X are the accepted and mean values, respectively.

The t_{exp} values for vanillin syrup (Sample 1) and vanillin powder (Sample 2) samples were calculated as 2.20 and 1.15, respectively, which are smaller than $t_{\text{critical}} =$

Table 2. The obtained results for the analysis of vanillin content in vanillin samples ($n=3$).

Food Sample	Labeled Content	Found with Std. Add.- Amp. Method (%)	Found UV-Vis Method (%)
Vanillin Syrup	25.00 %	25.10 \pm 0.08 $t_{\text{exp}} = 2.20$	24.50 \pm 0.15 $t_{\text{exp}} = 2.30$
		$F = 3.52$	
Vanillin Powder	3.00 %	3.02 \pm 0.03 $t_{\text{exp}} = 1.15$	2.95 \pm 0.07 $t_{\text{exp}} = 0.99$
		$F = 5.44$	
		$t_{\text{critical}}: 4.30$ (P:0.05, 2), $F_{\text{critical}}: 19$ (P:0.05, 2, 2) [32]	

2.78 (Confidence level = 95 % and degrees of freedom = 2) [32]. In this connection, it can be concluded that there is no significant difference between μ and X , and the null hypothesis may be accepted. Also, the alternative and null hypotheses were identified as $H_A: s_1^2 \neq s_2^2$ and $H_0: s_1^2 = s_2^2$ for the F-test and s_1^2 and s_2^2 are the variances of the proposed method and UV-Vis method, respectively. The experimental F values for syrup and powder samples were calculated as 3.52 and 5.44, which are lower than the F_{critical} value (19) [32]. As a result, the null hypothesis may be accepted. The results of F tests confirm that there is no significant difference between the standard deviations of the two mentioned methods.

4 Conclusion

In the proposed study, a simple, accurate, selective, and sensitive amperometric determination of vanillin based on Cu/ITO was described. The Cu particles bring a good conductive property to the ITO and the modified electrode exhibits a good electrocatalytic effect towards the oxidation of vanillin. Amperometric measurements indicated that the electrocatalytic oxidation current belongs to vanillin increased linearly between 0.50 μM –2.0 mM. The LOD was determined as 0.15 μM . According to the obtained results, the Cu particles were found to be a suitable electrode modification material for sensitive, accurate, and selective amperometric determination of vanillin detection. Besides, the Cu/ITO exhibits good repeatability and reproducibility towards the determination of vanillin. Finally, the applicability studies confirmed that the proposed method provides amperometric determination of vanillin in high accuracy and precision.

Data Availability Statement

Data sharing not applicable- no new data generated.

References

- [1] J. Peng, W. Liying, Y. Liu, W. Zhuge, Q. Huang, W. Huang, G. Xiang, C. Zhang, *RSC Adv.* **2020**, *10*, 36828–36835.
- [2] L. Fu, K. Xie, D. Wu, A. Wang, H. Zhang, Z. Ji, *Mater. Chem. Phys.* **2020**, *242*, 122462.
- [3] C. Raril, J. G. Manjunatha, *Microchem. J.* **2020**, *154*, 104575.
- [4] T. Zabihpour, S.-A. Shahidi, H. Karimi-Maleh, A. G.-H. Saraei, *J. Food Meas. Charact.* **2020**, *14*, 1039–1045.
- [5] Y. Tian, P. Deng, Y. Wu, J. Liu, J. Li, G. Li, Q. He, *Microchem. J.* **2020**, *157*, 104885.
- [6] S. Karakaya, *Monatsh. Chem.* **2019**, *150(11)*, 1911–1920.
- [7] B. Aslışen, Ç. C. Koçak, S. Koçak, *Anal. Lett.* **2020**, *53*, 343–354.
- [8] S. Karakaya, İ. Kaya, *Polymer* **2021**, *212*, 123300.
- [9] B. Thirumalraj, C. Rajkumar, S. M. Chen, N. Dhenadhayan, K. C. Lin, *ChemElectroChem* **2017**, *4*, 2842–2851.
- [10] L. Huang, K. Hou, X. Jia, H. Pan, M. Du, *Mater. Sci. Eng. C* **2014**, *38*, 39–45.
- [11] Q. Mei, Y. Ding, L. Li, A. Wang, Y. Zhao, *J. Electroanal. Chem.* **2019**, *33*, 297–303.
- [12] Y. Yardım, M. Gülcan, Z. Şentürk, *Food Chem.* **2013**, *141*, 1821–1827.
- [13] N. Alpar, Y. Yardım, Z. Şentürk, *Sens. Actuators B* **2018**, *257*, 398–408.
- [14] G. M. Durán, E. J. Llorent-Martínez, A. M. Contento, Á. Ríos, *Microchim. Acta* **2018**, *185*, 204.
- [15] P. Prabhu, R. S. Babu, S. S. Narayanan, *J. Mater. Sci. Mater. Electron.* **2019**, *30*, 9955–9963.
- [16] S. Peshoria, A. K. Narula, *J. Mater. Sci. Mater. Electron.* **2018**, *29*, 13858–13863.
- [17] R. Pruna, A. Baraket, A. Bonhommé, N. Zine, A. Errachid, M. López, *Electrochim. Acta* **2018**, *283*, 1632–1639.
- [18] B. Zhang, Q. Wu, B. Li, X. Tang, F. Ju, Q. Q. Yang, Q. Wang, Y. L. Zhou, *Int. J. Electrochem. Sci.* **2020**, *15*, 137–148.
- [19] A. Benvidi, P. Kakoolaki, H. R. Zare, R. Vafazadeh, *Electrochim. Acta* **2011**, *56*, 2045–2050.
- [20] H. R. Zare, S. Hossein Hashemi, A. Benvidi, *Anal. Chim. Acta* **2010**, *668*, 182–187.
- [21] M. Zhu, R. Li, M. Lai, H. Ye, N. Long, J. Ye, J. Wang, *J. Electroanal. Chem.* **2020**, *857*, 113730.
- [22] S. Yang, G. Zang, Q. Peng, J. Fan, Y. Liu, G. Zhang, Y. Zhao, H. Li, Y. Zhang, *Anal. Chim. Acta* **2020**, *1104*, 60–68.
- [23] S. Ayaz, S. Karakaya, G. Emir, D. G. Dilgin, Y. Dilgin, *Microchem. J.* **2020**, *154*, 104586.
- [24] G. Suppan, M. Ruehrig, A. Kanitz, H. J. Gores, *ECS J. Electrochem Soc.* **2015**, *162(8)*, D382–D388.
- [25] S. Z. El Abedin, M. Pölleth, S. A. Meiss, J. Janek, F. Endres, *Green Chem.* **2007**, *9*, 549–553.
- [26] S. Pourbeyram, J. Abdollahpour, M. Soltanpour, *Mater. Sci. Eng. C* **2019**, *94*, 850–857.
- [27] A. Khan, A. Rashid, R. Younas, R. Chong, *Int. Nano Lett.* **2016**, *6*, 21–26.
- [28] J. Jin, H. Mei, H. Wu, S. Wang, Q. Xia, Y. Ding, *J. Alloys Compd.* **2016**, *689*, 174–181.
- [29] J. Peng, L. Wei, Y. Liu, W. Zhuge, Q. Huang, W. Huang, G. Xiang, C. Zhang, *RSC Adv.* **2020**, *10*, 36828–36835.
- [30] A. T. Ezhil Vilian, P. Puthiaraj, C. Hwan Kwak, S.-K. Hwang, Y. S. Huh, W.-S. Ahn, Y.-K. Han, *ACS Appl. Mater. Interfaces* **2016**, *8*, 12740–12747.
- [31] P. Deng, Z. Xu, R. Zeng, C. Ding, *Food Chem.* **2015**, *180*, 156–163.
- [32] A. S. Douglas, D. M. West, F. J. Holler, *Fundamentals of analytical chemistry*, 5th Edition, **1988**, New York: Sanders Collage Publishing.

Received: January 3, 2021

Accepted: March 19, 2021

Published online on March 31, 2021